Marine Pollution Bulletin 221 (2025) 118520

Contents lists available at ScienceDirect

Marine Pollution Bulletin

journal homepage: www.elsevier.com/locate/marpolbul

Impact of desalination on the general circulation of the Arabian Gulf: Present and future scenarios

Maryam R. Al Shehhi [a,*], Hajoon Song [b,*], Jeffery Scott [c], Fahim Abdul Gafoor [a], John Marshall [c]

[a] Department of Civil and Environmental Engineering, Khalifa University of Science and Technology, Abu Dhabi, United Arab Emirates
[b] Department of Atmospheric Sciences, Yonsei University, Seoul, Republic of Korea
[c] Earth, Atmospheric and Planetary Science Department, Massachusetts Institute of Technology, 77 Massachusetts Ave., Cambridge, MA 02139, USA

ARTICLE INFO

Keywords:
Brine discharge
Desalination
Ocean impacts
Sea of Oman
Indian Ocean
Saline outflow
MITgcm

ABSTRACT

By 2050, freshwater production by desalination plants is projected to increase more than sixfold compared to today's levels. Hundreds of seawater desalination plants currently operate in the Arabian Gulf, and the regional and local responses to brine discharge can be significant, especially on the Arabian coast in the southwestern Gulf. Here, we use a 2.5 km-resolution ocean model of the Gulf and the Sea of Oman to investigate the impact of increased salinity on circulation and water mass transformation within the Gulf under desalination forcing scenarios ranging from no desalination to an extreme 50-times present levels (50×). As forcing intensifies, salty, warm, dense waters sink to the bottom of the Gulf, leading to increases in salinity and temperature, with the most extreme scenario showing subsurface temperature and salinity near the southern shoreline rising by approximately 0.6 °C and 2 g/kg, respectively. With increasing forcing, we find stronger surface inflow of fresher water through the Strait of Hormuz and stronger outflow of warm, salty water into the Sea of Oman. The efficient exchange of water between the interior Gulf and the Sea of Oman, enhanced by brine discharge, strengthens and deepens through the Strait of Hormuz, increasing inflow and outflow rates by 20 % and effectively muting large-scale changes in temperature and salinity, even under extreme desalination scenarios. Impacts are much larger near desalination plants, with altered surface and subsurface flow patterns, increased mass transformation, and strengthened meridional and zonal overturning circulation.

Key findings

1. Salinity and Temperature Rise: Extreme (50×) desalination increases subsurface temperature by 0.6 °C and salinity by 2 g/kg near the southern Gulf shoreline.
2. Enhanced Water Exchange: Brine discharge boosts inflow/outflow through the Strait of Hormuz by 20 %, limiting large-scale temperature/salinity changes.
3. Local Circulation Changes: Near desalination plants, flow patterns shift, with stronger mass transformation and overturning circulation.

1. Introduction

Due to limited freshwater resources, many countries depend on desalination plants to provide fresh water for domestic and industrial purposes. Although such plants meet an urgent need, insufficient dilution of salty discharge into the marine environment can negatively affect marine habitats such as corals and seaweed meadows (Danoun, 2007). Around half of the world's desalination plants are located in the arid regions of the Middle East, surrounding the Arabian Gulf (Roberts et al., 2010; Hosseini et al., 2021), which has an estimated desalination capacity of 11 million m^3 day^{-1} (Uddin, 2014). This production capacity comes from hundreds of active desalination plants, ranging from small-scale to large-scale plants, primarily along the shallow western and southern shore of the Gulf (Ibrahim et al., 2020), and many additional ones are expected to be commissioned in the near future (Sharifinia et al., 2019; Hosseini et al., 2021; Purnama, 2021). With an increasing population in the Arabian Gulf region, desalination capacity is projected to grow significantly to meet rising water demand. However, this expansion does not necessarily imply a proportional increase in the number of plants, as technological advancements allow for higher production efficiencies in existing facilities (Rasoulpour and Akbari, 2024). As shown in Fig. 1, the cumulative projected desalination capacity in 2050 is 80 million m^3 day^{-1} which is more than double that in 2020 and

* Corresponding authors.
E-mail addresses: maryamr.alshehhi@ku.ac.ae (M.R. Al Shehhi), hajsong@yonsei.ac.kr (H. Song).

https://doi.org/10.1016/j.marpolbul.2025.118520
Received 19 September 2024; Received in revised form 28 July 2025; Accepted 28 July 2025
Available online 2 August 2025

eight times that in 2010 (Le Quesne et al., 2021; Saif, 2012). Although seawater desalination is an effective solution to the scarcity of fresh water, it puts pressure on the marine ecosystem especially in coastal areas. The salinity of brine discharge in the Arabian Gulf is typically higher than the ambient seawater, often reaching up to 1.7 times its natural salinity. Given that the Gulf's seawater salinity is approximately 39–45 psu, brine discharge can range from 50 to 66 psu or higher in some cases (Shim et al., 2017; Alosairi et al., 2018). Since the density of

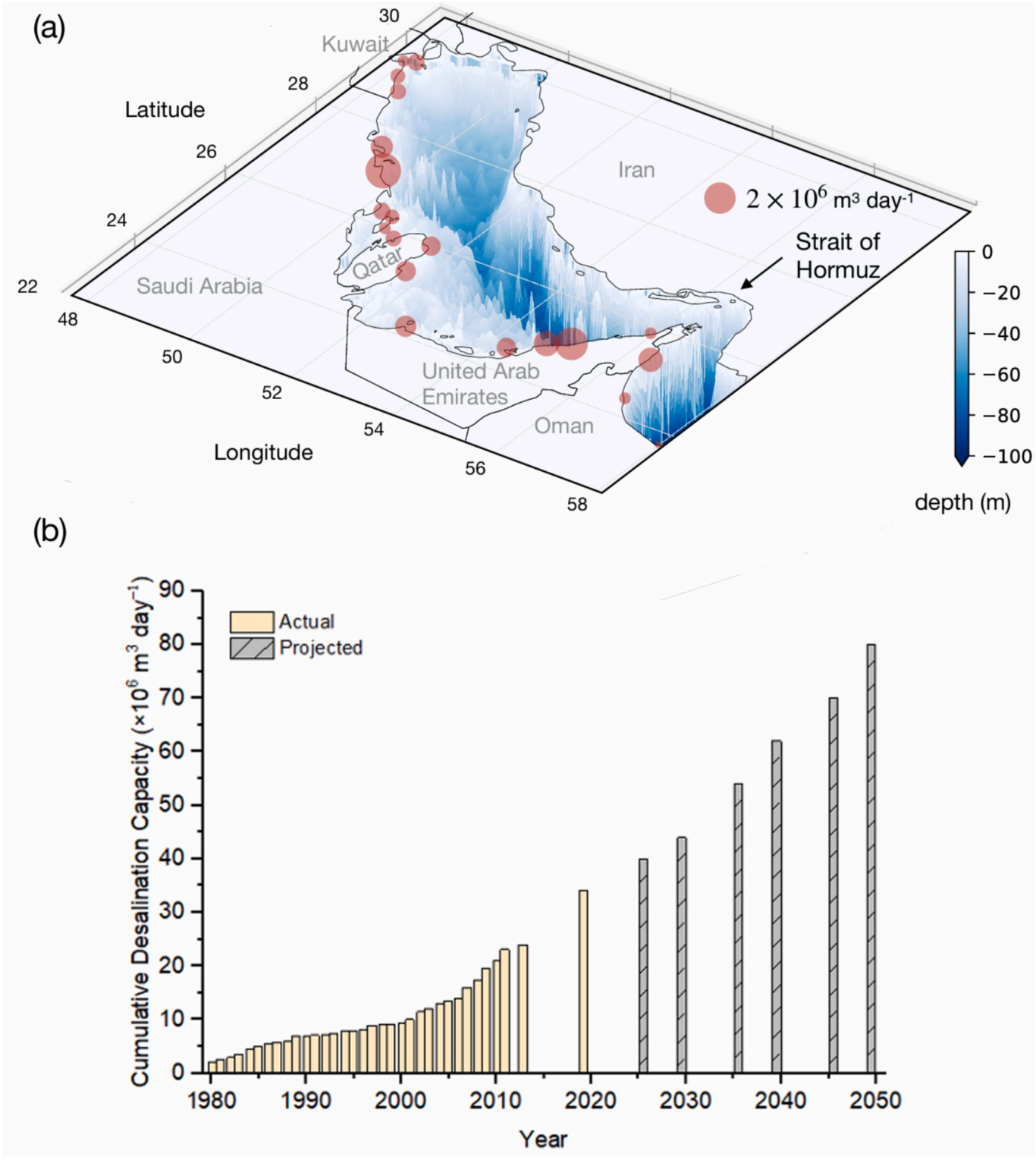

Fig. 1. (a) The location of major desalination plants along the coast of the Arabian Gulf are presented by the red circles. The size of the circles corresponds to the capacity of freshwater produced from each desalination plant. Blue represents the bathymetry of the Gulf, ranging from shallow (shaded light) waters to 100 m deep (shaded dark). (b) Cumulative desalination capacity around the Arabian Gulf (1×10^6 m^3 day^{-1}) between 1980 and 2020 and the projection between 2020 and 2050. The desalination plant dataset was obtained from the DesalData database (http://www.desaldata.com). (For interpretation of the references to color in this figure legend, the reader is referred to the web version of this article.)

discharge is largely determined by its salinity, it typically sinks (Einav et al., 2003). However, before reaching the bottom, horizontal tidal mixing and transport processes can contribute significantly to its initial dispersion (Alosairi et al., 2018). Since discharge takes place in a coastal zone in the presence of complex ocean currents (Ruso et al., 2007; Sola et al., 2020), waters can sink to the bottom and spread along the seabed, the details depending on outfall design and the mixing and flushing characteristic of the local area. Note also that brine outflows from desalination plants can exceed seawater ambient temperature (Missimer and Maliva, 2018), depending on the desalination technology employed. However, for simplicity we do not attempt to capture temperature changes here and instead focus on understanding the non-local impacts of increased salinity associated with desalination activities.

Most environmental impact studies have been conducted primarily to assess effects local to the desalination plants rather than broader regional changes. For example, studies have found salinity increases up to 2 psu at distances of 20 m from the outlet, decaying to 0.8 psu at a distance of 100 m or so (Roberts et al., 2010; Clark et al., 2018), with concomitant temperature increase up to 0.7 °C (Kress et al., 2020). However, individual outfalls have individual footprints, which depend on flow rates, effluent characteristics and outfall design. There have been fewer studies of the wider implications of desalination on the large-scale circulation of the Gulf. Ibrahim & Eltahir (2019) used a high-resolution coupled Gulf Atmosphere Regional Model (GARM) and found that flushing by the residual circulation inhibited salt buildup on the scale of the basin. Campos et al. (2020) found that velocities in the deep channel of the Strait of Hormuz increased by 0.20 m s^{-1} when the impact of brine discharge is considered. Paparella et al. (2022) modeled the impact of desalination plants on the Gulf using atmospheric forcing based on the IPCC SSP5–8.5 scenario which yielded reduced evaporation rates, increased air temperature, and higher precipitation in the Arabian Gulf. They found that it is unlikely for the average salinity to increase by more than 1 psu and, under less extreme scenarios, will likely remain well below 0.5 psu, with negligible environmental impacts.

Progress has been made in understanding the large-scale implications of salinization on the oceanography of the Gulf. However, further research is needed to address remaining gaps and deepen our understanding of its broader impacts including how desalination affects water mass transformation going on within the Gulf, the associated vertical overturning circulation and the exchange with the Sea of Oman through the Strait of Hormuz. Here we also address extreme scenarios in which desalination rates are increased 50-fold (×50). By exploring extreme cases we can study the system's resilience to environmental stressors and the key ways in which the Gulf might change. To that end we take a high-resolution model of the circulation of the region with a good and documented climatology – the model is described in Al-Shehhi et al. (2021) – and perturb it with salinity sources associated with the desalination plants shown in Fig. 1. We then hypothesize that the desalination stress on the ocean is increased 10-fold, 20-fold etc. and, in an extreme case, up to 50-fold over present-day values. We document how circulation, stratification, hydrography and exchange properties change relative to the unperturbed state, and the patterns of those changes.

2. Modeling framework and implementation

2.1. Model setup

The high resolution three-dimensional hydrodynamic model of the Arabian Gulf described in Al-Shehhi et al. (2021) is used in this study. It is based on the Massachusetts Institute of Technology's general circulation model (MITgcm) (Marshall et al., 1997). The model domain extends from the Arabian Gulf to the Sea of Oman. The model bathymetry is obtained from the 1-min Smith and Sandwell Global Topography dataset (Smith and Sandwell, 1997) as indicated by the blue shading in Fig. 1. The MITgcm employs a finite-volume discretization methodology, with the governing equations formulated in z-coordinates. The model grid has a quasi-uniform horizontal resolution of 2.5 km with 83 vertical layers, which are designed to be much thinner near the surface (~1 m) to better resolve upper ocean dynamics and progressively thicker at greater depths to capture deep-water processes. There are 25 layers in the Gulf. Initial and boundary values of zonal and meridional velocity components, temperature, salinity, and sea surface height were obtained from a global ocean MITgcm simulation LLC4320 with the same resolution in horizontal and vertical (Rocha et al., 2016). Boundary conditions were imposed at the southern and eastern boundaries in the Sea of Oman including surface elevation and currents associated with eight tidal constituents (K2, S2, M2, N2, K1, P1, O1, Q1) derived from a global tidal model (Tidal Prediction eXternal Software: TPXO) (Egbert et al., 1994). The model was driven by 6-hourly atmospheric forcing data from the European Centre for Medium-Range Weather Forecasts (ECMWF) at a spatial resolution of 0.14° (Hersbach et al., 2020). The reanalysis data includes downward short and longwave radiation, precipitation, wind components at a height of 10 m together with the 2 m temperature and dew point. Runoffs from four rivers – the Shatt Al-Arab, Hendijan, Hilleh, and Mand – are also included (Alosairi and Pokavanich, 2017). The simulation represents the repeating year 2012, following a 6-year spin-up period, by which point the model has reached a state independent of its initial conditions.

2.2. Climatology

The climatology of the model is documented in detail in Al-Shehhi et al. (2021), where it is compared with a range of observations, both in-situ and remotely sensed. We show some key aspects of the model climatology in Fig. 2. The simulated annual mean sea surface temperature (SST) varies from 22 °C in the north to 28 °C in the southeastern region of the Gulf toward the Sea of Oman (Fig. 2(a)). The surface annual-mean salinity (S) presented in Fig. 2(b) reveals that, as expected, the interior Gulf is generally saltier than the waters of the Sea of Oman and is the saltiest in the inner Gulf and along the south coast where salinity can exceed 45 psu (g/kg). This pattern is also observed at the bottom, reflecting the high salinity throughout the water column in these regions. This reflects the fact that the Gulf is an evaporative basin and the inflow through the Strait of Hormuz comprises relatively fresh water.

Fig. 2(c,d) show the residual overturning circulation in the zonal and meridional planes, respectively. The residual overturning circulation represents the flow patterns responsible for tracer transport and can be accurately estimated in density space. It is derived through either meridional or zonal integration of the velocity, weighted by the grid intervals in density space, before converting to depth coordinate for improved readability. Detailed processes can be found in Al-Shehhi et al. (2021). In the zonal vertical plane, we observe water being drawn into the Gulf at the surface and out at depth (negative indicates anticlockwise circulation in the zonal vertical plane). The circulation in the zonal plane (surface inflow and outflow at depth) aligns with previous observational studies (e.g., Reynolds, 1993; Johns et al., 2003). In the meridional plane, there is also a tendency for water to upwell in the central Gulf and then move southward toward the south coast where it sinks to depth before outflowing through the Strait of Hormuz, consistent with the findings of Thoppil and Hogan (2010). The underlying dynamics and associated water mass transformation is described in Al-Shehhi et al. (2021). The ability of the model to represent tides and their role in the general circulation are also described in (Salim et al., 2024) and (Subeesh et al., 2025). This base model is now perturbed by various desalination scenarios and changes monitored and documented. The initial conditions are the same in each scenario.

2.3. Desalination scenarios

We have implemented six desalination scenarios: no desalination

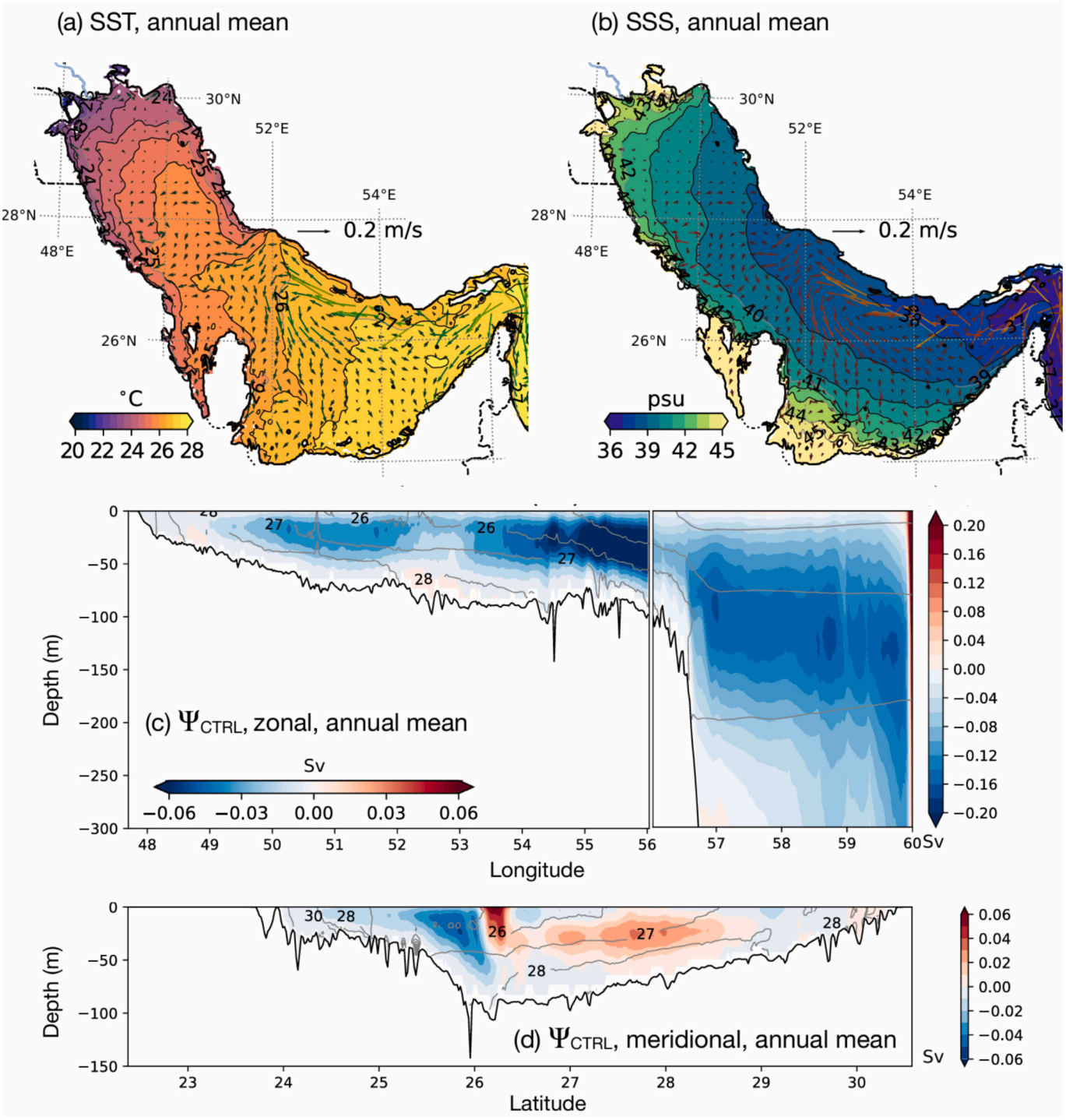

Fig. 2. The mean (a) SST and (b) SSS with the surface current from the climatology simulation. (c) and (d) are the mean zonal and meridional residual overturning streamfunction (Ψ), respectively. It is noted that the color scales of the zonal residual streamfunction in (c) are different in the Arabian Gulf and the Sea of Oman. There is anticlockwise (clockwise) circulation around the blue (red) streamfunction. (For interpretation of the references to color in this figure legend, the reader is referred to the web version of this article.)

activities (CTRL), 1-fold (×1, with salinity forcing implemented to mimic plants shown in Fig. 1), 10-fold (×10), 20-fold (×20), 35-fold (×35) and a 50-fold (×50) increase in forcing. To estimate local salinity impacts from desalination plants, we used reported plant brine discharge rates (Alosairi and Pokavanich, 2017) and assumed that the freshwater removal rate was equal to the discharge rate (in essence, a freshwater recovery rate of 50 %). Note this is a somewhat higher removal rate than is typically achieved (which is in the range 15–40 %) (Lattemann and Höpner, 2008). Each of the six scenarios was spun up for a period of 6 years. Moreover, in reality some of the freshwater produced is returned to the Gulf in the form of wastewater. We should therefore interpret our forcing as an "upper bound" of the true desalination impact, in keeping with the idealized, broad nature of our study. Desalination forcings were implemented by changing the applied E-P-R (evaporation, precipitation, runoff) at desalination plant locations corresponding to the red circles shown in Fig. 1. One way of thinking of this

is that the desalination plants are being represented as "negative freshwater rivers", in order to mimic the effects of brine discharge. As noted previously, no attempt is made to represent any direct temperature effect of the desalination plants. Fig. 3 is a schematic diagram presenting the framework implemented.

It should be noted that the map of desalination plants used here (Fig. 1) is taken from Ibrahim et al. (2020) and captures more than 93 % of current desalination plants. However, smaller plants on the eastern/northern coasts of the Gulf - see Rasoulpour and Akbari (2024) - are unfortunately not included but should be in future studies. That said, our goal is to explore the large-scale impact of desalination across a broad range of amplitudes rather than simulate in detail the contribution of individual plants.

3. Impact of salinity forcing on the circulation, hydrography and overturning circulation in the Gulf

We first discuss changes in the large-scale pattern of currents and exchange between the Gulf and the Sea of Oman through the Strait of Hormuz. We go on to discuss changes in the temperature and salinity properties of the Gulf and its zonal and meridional overturning circulations.

3.1. Surface ocean currents and exchange

The desalination plants result in anomalous surface and bottom currents in the Gulf, and the size of anomalies increases with the capacity of the desalination plants (Figs. 4(a–d) and 5(a–d)). In ×10, we observe anomalous gyres near the northern, deeper parts of the Gulf (26°N-28°N and 52°E-54°E), which are consistent with those described by Thoppil and Hogan (2010) along the Iranian coast. However, these gyres appear to be intensified in our analysis, likely due to the influence of brine discharge from desalination plants, which enhances density-driven circulation in the region. There are also anomalous surface flows toward the sites of desalination plants (Fig. 4(a,b)). The brine discharge increases salinity near the outfall areas, and the resulting dense, salty water sinks to depth, creating a pronounced density gradient. This gradient draws fresher surface water from the northern Gulf toward the region, enhancing the strength of both horizontal and vertical circulations along the south coast (offshore of the UAE). They are more evident in the ×50 case, showing enhanced inflow through the Strait of Hormuz into Gulf along the northern coast before flowing toward the desalination plants (Fig. 5(a,b)). The size of these anomalous flows can be substantial, approximately 50 % of the surface current in CTRL.

The anomalous bottom currents in the Gulf generally flow out from the desalination plants toward the Strait of Hormuz (Figs. 4(c,d) and 5(c,d)). These currents are strongest near the desalination plants and flow down bathymetric slopes. Again, anomalous bottom currents are more pronounced in ×50, which carry the warm, salty water mass out to the Sea of Oman. Hence, the desalination plants have the potential to 'draw' surface waters in toward them, where it is made dense and sinks before moving away from the sites toward the Strait of Hormuz.

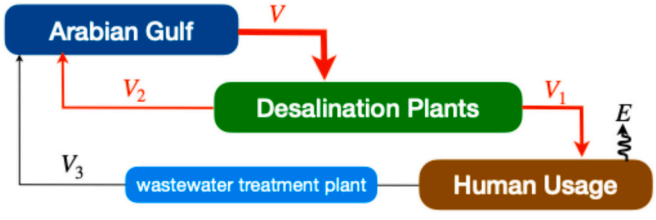

Fig. 3. Desalination plants extract seawater of volume V from the Arabian Gulf, producing freshwater of volume V_1 and returning warm, salty water of volume V_2 back to the Gulf. Some of the freshwater re-enters the Gulf as wastewater or local precipitation following evaporation (E). Taking the collective red arrows into consideration, the removal of freshwater of volume V_1 is accomplished through negative river runoff as a forcing, i.e., in the ocean model effectively only implementing arrow V but at a reduced flow rate. (For interpretation of the references to color in this figure legend, the reader is referred to the web version of this article.)

As the imposed salinity forcing increases, we observe stronger outflow of saltier, warmer and denser waters from the Gulf into the Sea of Oman through the Strait of Hormuz, which is balanced by stronger inflow of relatively fresher, cooler waters (Figs. 4(e–g) and 5(e–g)). Vertical cross-sections through the Strait of Hormuz reveal that anomalously salty water exits the Gulf at depth on the southern side of the Strait, with fresher water being drawn in to the north near the surface. This pattern aligns with the 'normal' estuarine circulation previously described in the literature (e.g., Thoppil and Hogan, 2010; Johns et al., 2003). However, our analysis indicates that the inflow and outflow are intensified compared to baseline conditions, likely due to the enhanced density gradient driven by brine discharge from desalination plants. The main changes are in the salinity and exchange. This anthropogenic forcing reinforces the exchange through the Strait, amplifying both the inflow of fresher water and the outflow of salty water. The anomalies are most pronounced toward the bottom because the products of the desalination plants are salty and dense.

3.2. Temperature and salinity

The impact of desalination plants on the surface and bottom S and T grows with the capacity of the desalination plants. At present day levels of desalination (×1) there is limited impact on the surface and bottom S and T (not shown). As desalination rates increase to 10-fold (×10), the SST changes are still less than 0.2 °C in the Gulf, while there is a tendency to cool in the eastern part of the Gulf (Fig. 4(a)). This is likely due to cooler water being drawn into the Gulf from the Sea of Oman through the Strait of Hormuz due to the enhanced density gradient. In addition, there is a noticeable increase in the bottom temperature by more than 1 °C associated with brine discharge near desalination plants, which is advected away toward deeper regions (Fig. 4(c)).

In the extreme 50-fold case (×50), we see a distinct line – what may be called a 'flushing line' – along which warm (and salty) waters leave the Gulf (Fig. 5(c)). The temperature anomalies at the surface are comparable with those in ×10, showing generally less than 0.2 °C in the Gulf (Fig. 5(a)). However, the bottom temperature anomalies exceed 2 °C near the sites of desalination plants and gradually decreases along the flushing line as the water mass moves away (Fig. 5(c)). This suggests that there is an active source of warm water at the desalination plants which flows out of the Gulf mainly along the slope of bathymetry. There is also significant increase of temperature near the southern part of the Strait of Hormuz, suggesting that the temperature of the outflow is increased by up to 1 °C.

The salinity anomalies reveal clear patterns caused by brine discharge. In ×10, the surface salinity anomalies increase reaching their maximum along the southern shoreline: 0.5–2 psu, and exceeding 2 psu to the east of Qatar (Fig. 4(b)). To the south of Bahrain, near the Gulf of Salwa, surface salinity averages about 8 psu and can exceed 10 psu in some areas. The bottom salinity increases even more, showing broader areas where salinity anomalies exceed 0.5 psu along the southern shoreline (Fig. 4(d)). The positive salinity anomalies extend to the southern part of the Strait of Hormuz, showing the exit of salty waters into the Sea of Oman.

The positive salinity anomalies are significant in the 50-fold scenario, particularly near the bottom of the Gulf (Fig. 5(b,d)). At the surface, waters coming into the Gulf and approaching desalination plants have salinity anomalies which can exceed 2 psu (Fig. 5(b)). The bottom salinity anomalies significantly exceed 2 psu near the desalination plants. This salty water flows eastward, eventually leaving the Gulf through the southern part of the Strait of Hormuz (Fig. 5(d)). Again, the region on the west, close to Qatar exhibits a salinity increase which is

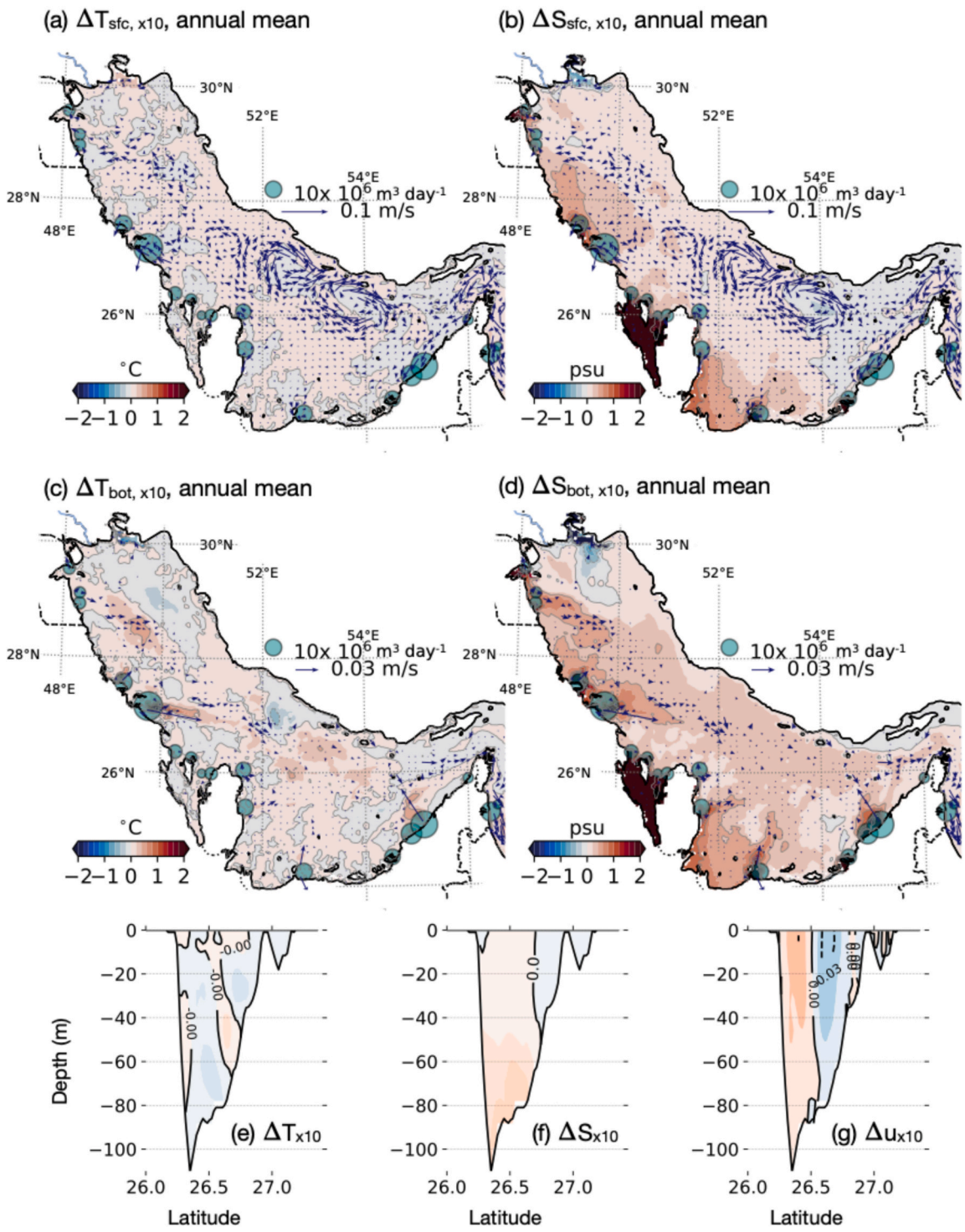

Fig. 4. Changes of (a) SST, (b) SSS, (c) bottom temperature and (d) bottom salinity between ×10 and CTRL are color shaded, while arrows represent changes in flow at those levels. (e–f) show anomalies of T, and zonal flow, respectively, at the Strait of Hormuz. The circles in (a–d) represent the capacity of the desalination plants in ×10 simulation.

much larger than 2 psu because of poor flushing as evidenced by the anomalous current flowing toward the coast.

The magnitude of salinity and temperature anomalies generally increases with depth, resulting in stronger stratification (Fig. 6). The increase of the vertical stability is particularly significant in ×50 where the bottom density increases approximately 1 kg/m^3, while the surface density rises by less than 0.5 kg/m^3. This is primarily driven by the increase of salinity. The median salinity near 100 m is nearly 1.5 psu greater in ×50 than in CTRL, which is more than three times the size of anomaly at the surface. This is somewhat expected as the desalination plants transform the water mass toward higher density classes and so their impact accumulates near the bottom of the Gulf. These changes also suggest that the increasing capacity of the desalination plants in the Gulf exerts higher pressure on the marine environment near the bottom. While many benthic Gulf species are adapted to hypersaline conditions, the additional salinity increase from brine discharge, often greater than

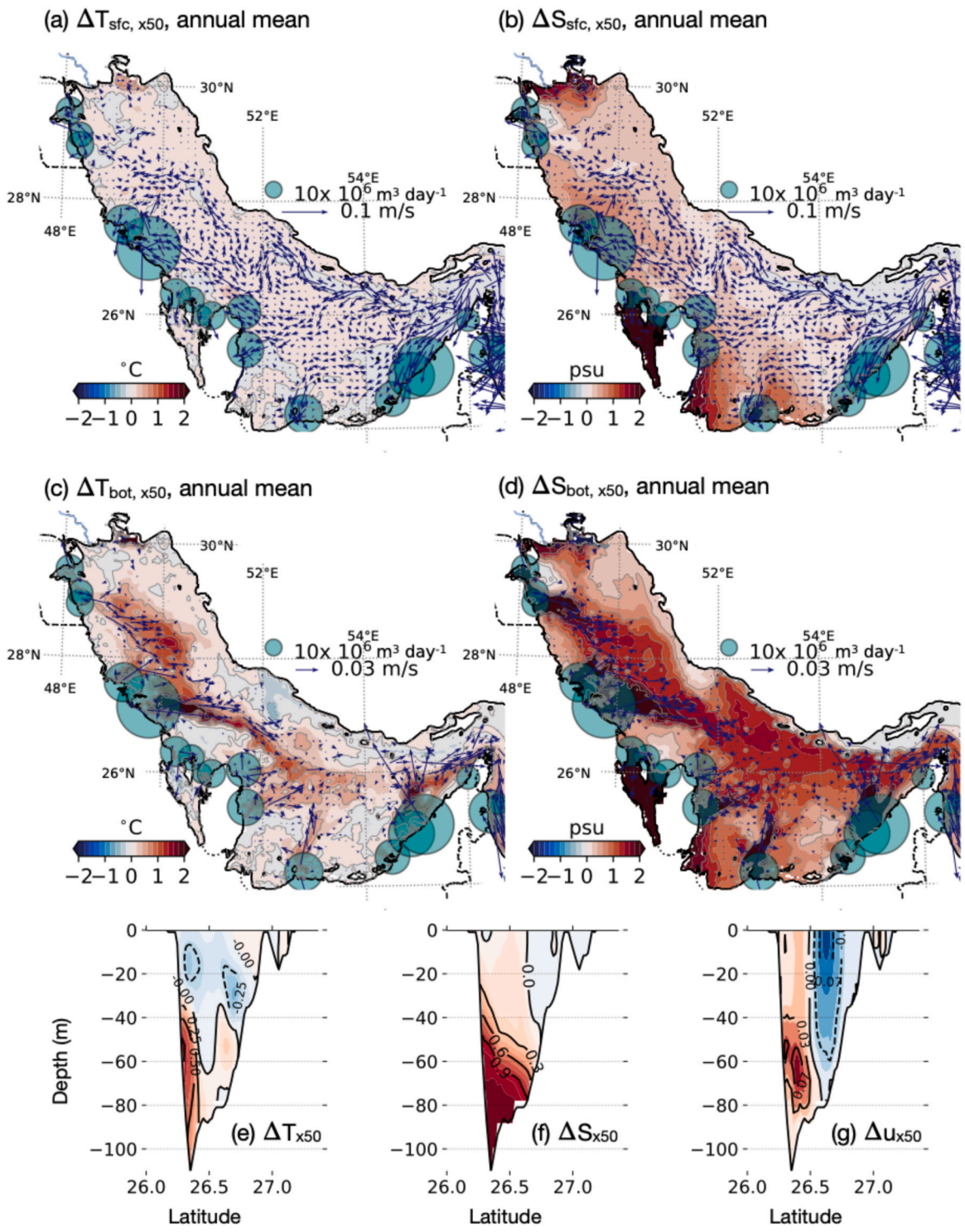

Fig. 5. Same as Fig. 4, except the changes are between ×50 and CTRL.

3 g/kg in localized areas, may exceed the tolerance thresholds of sensitive benthic organisms. This might result in habitat loss, shifts in community structure, and reduced biodiversity in affected areas (Roberts et al., 2010).

3.3. Changes in overturning circulation

Upon introduction of local salinity forcing from desalination plants, comparison of the anomaly from ×50 in Fig. 7(a,b) with the CTRL in Fig. 2(c,d), shows that the patterns and sense of the overturning circulation – both in the meridional and zonal directions – remains the same but becomes stronger. Measures of the strength of these overturning circulations as a function of desalination strength is plotted in Fig. 7(c,d). Most changes occur in the northern and western regions of the Gulf. We observe a broad increase in the strength of these overturning cells, and the change does not 'level out' even for ×50, at which point overturning strength approaches 50 % of the mean. This supports the 'flushing' hypothesis of Ibrahim and Eltahir (2019) that the Gulf can efficiently exchange waters with the Sea of Oman buffering interior change.

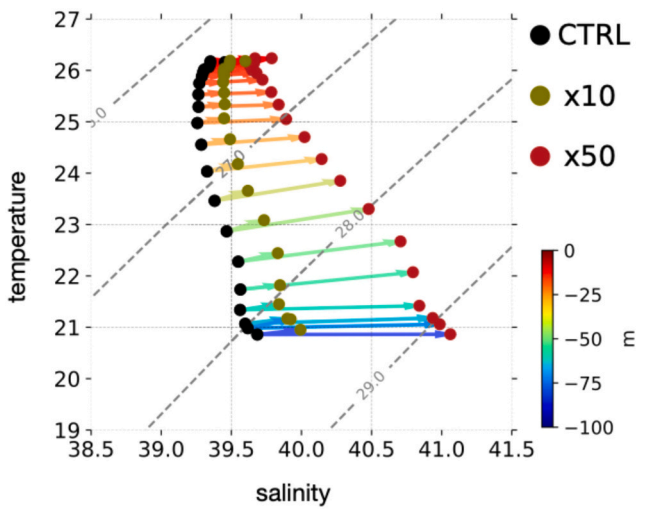

Fig. 6. The median values of temperature and salinity in CTRL (black dots), ×10 (olive dots) and ×50 (red dots) at each vertical level. The arrows and their colors represent changes of water properties as a function of desalination forcing and depth, respectively. (For interpretation of the references to color in this figure legend, the reader is referred to the web version of this article.)

Interestingly, the overturning circulation in the Sea of Oman has also intensified in ×50 (Fig. 7(a)). This change is greater than in the Gulf, showing approximately a 100 % increase compared to CTRL (Fig. 7(f)). The anomalous streamfunction extends deeper than 200 m in the Sea of Oman, indicating that the outflow from the Gulf can sink deeper in ×50 than in CTRL due to the increased salinity of Gulf outflow. At the surface, the westward flow toward the Gulf is intensified with increased desalination capacity. Hence, the enhanced overturning circulation in the Sea of Oman supports a more efficient exchange of the water in the Gulf.

3.4. *Changes in the water-mass transformation rates*

Quantification of the water mass transformation rate – that is the rate at which the density of water is changed from one value to another – is discussed at length in Al Shehhi, 2021 for our CTRL scenario in which any local (desalination plant) salinity forcing was absent. In the annual-average, the Gulf has a positive water-mass transformation rate both by surface heat and freshwater fluxes (Fig. 8(a,b)), meaning that water is converted from lighter density classes to heavier ones. The largest contribution for the positive transformation rate is the latent heat flux followed by longwave radiation (Fig. 8(c)). In the Gulf, evaporation exceeds precipitation (the latter is negligible) thus increasing the density of surface waters in the Gulf. The shortwave radiation, however, lowers the density which largely compensates for the density increase by both longwave and latent heat flux combined, leading to both positive and negative values in the Gulf. On the other hand, the density increase by the freshwater flux is positive in most parts of the Gulf, resulting in greater contribution to the total water mass transformation rate.

The introduction of forcing does not change the broad pattern of water mass transformation. However, there are significant increases, by as much as 100 m^3/s, close to the desalination plants (not shown). When integrated over the whole Gulf, desalination plants rarely alter the water mass transformation rate contributed by heat and freshwater fluxes. In ×50, however, the contribution from a few desalination plants to the transformation rate becomes comparable to that of evaporation over the whole Gulf region (Fig. 8(c)). The increasing transformation rate due to desalination is consistent with the pattern of anomalous surface currents: the positive anomalies in the transformation rates (or increased diapycnal volume flux toward higher density) align well with the anomalous surface current observed in ×10 and ×50 (see Figs. 4(a,b) and 5(a,b)).

The positive water mass transformation rate due to diffusive salt flux below the surface layer can increase the density of the surface layer, though it is generally small compared to the surface buoyancy flux (Figs. 8(a,b) and 9(a)). However, in certain regions, larger localized transformation can occur where the KPP boundary layer mixing scheme can generate significantly enhanced localized diffusivities and mixing of salt. With the introduction of desalination plant forcings, the localized mixing of salt increases the density at the surface, particularly near the desalination plants in ×50 (Fig. 9(b)). The anomalous transformation rate by the salt mixing exceeds 100 m^3/s, and the contribution from diapycnal salt mixing to the surface layer density increase is greater than that from surface buoyancy fluxes. The positive anomalous transformation rate is also seen along the flushing line before the salty water from the desalination plants sinks away to depth. Given that the Gulf has a relatively uniform vertical profile in winter, this warm and salty water has the potential to increase the surface density.

4. Discussion

The overall impact of salinity forcing from desalination plants across the Arabian Gulf has been assessed through application of a 3D regional model based on the MITgcm. Four major rivers and several desalination plants in the Gulf region were considered in the six scenarios: no desalination plant forcing, existing scenario (1-fold), 10-fold, 20-fold, 35-fold and 50-fold increases. Our desalination plant forcing was found to increase the salinity by approximately 0.2 g/kg and over 3 g/kg along the Gulf coast for the entire Gulf in the most extreme scenario. Notable increases in salinity were observed in shallow regions near the coasts of Qatar and Bahrain where the circulation is weak and exchange with the interior Gulf limited. In addition, an increase in the depth-averaged temperature up to 0.2–1.0 °C near the discharge area of the desalination plants was noted, in Kuwait, Saudi and in the nearshore area of the United Arab Emirates. Seasonal variations in salinity and temperature were analyzed to understand the impacts of brine discharge under different stratification regimes. During the summer months, strong stratification suppresses vertical mixing, resulting in a significant increase in mean surface salinity and bottom temperature near the brine discharge sites. In contrast, winter conditions, characterized by weaker stratification, allow for more uniform mixing of brine throughout the water column, reducing the localized impact at the surface and bottom layers. Most of the impact of brine discharge on the salinity and temperature, however, occurs on regional scales within 2 to 3 km from where the discharge occurs. The offshore areas are less affected and response rather muted even in the most extreme desalination rates considered. An advantage of this study is the use of a CTRL simulation for direct comparison, which allows us to isolate and detect the desalination signal; otherwise, such signals are not easily distinguishable due to interannual variability and climate change influences. Temperature and salinity changes, even in the extreme ×50 desalination scenario considered here, are comparable to interannual changes in the Gulf but will likely be dwarfed by expected changes induced by anthropogenic warming over the current century (Lachkar et al., 2017). Unfortunately, the Gulf does not yet have adequate observing systems in place to monitor such variability, whatever their cause.

We also find impacts on the horizontal and vertical overturning circulations. As desalination rates are increased, fresher water is drawn into the Gulf more through the northern, surface regions of the Strait. This leads to an anticlockwise anomalous cell which returns waters mid-basin just north of the coastal shelf. Meanwhile salty waters are drawn over the shelf from the desalination plants operating on the southern coast. These sink to depth and exit the Gulf in a deep salty anomaly to the south of the Strait. The associated overturning circulations retain the same broad patterns but increase in strength reaching 50 % of the mean in the 50-fold scenario. This attests to the efficiency of the exchange which mutes the large-scale response of temperature and salinity. Therefore, we conclude that the large-scale circulation and patterns of

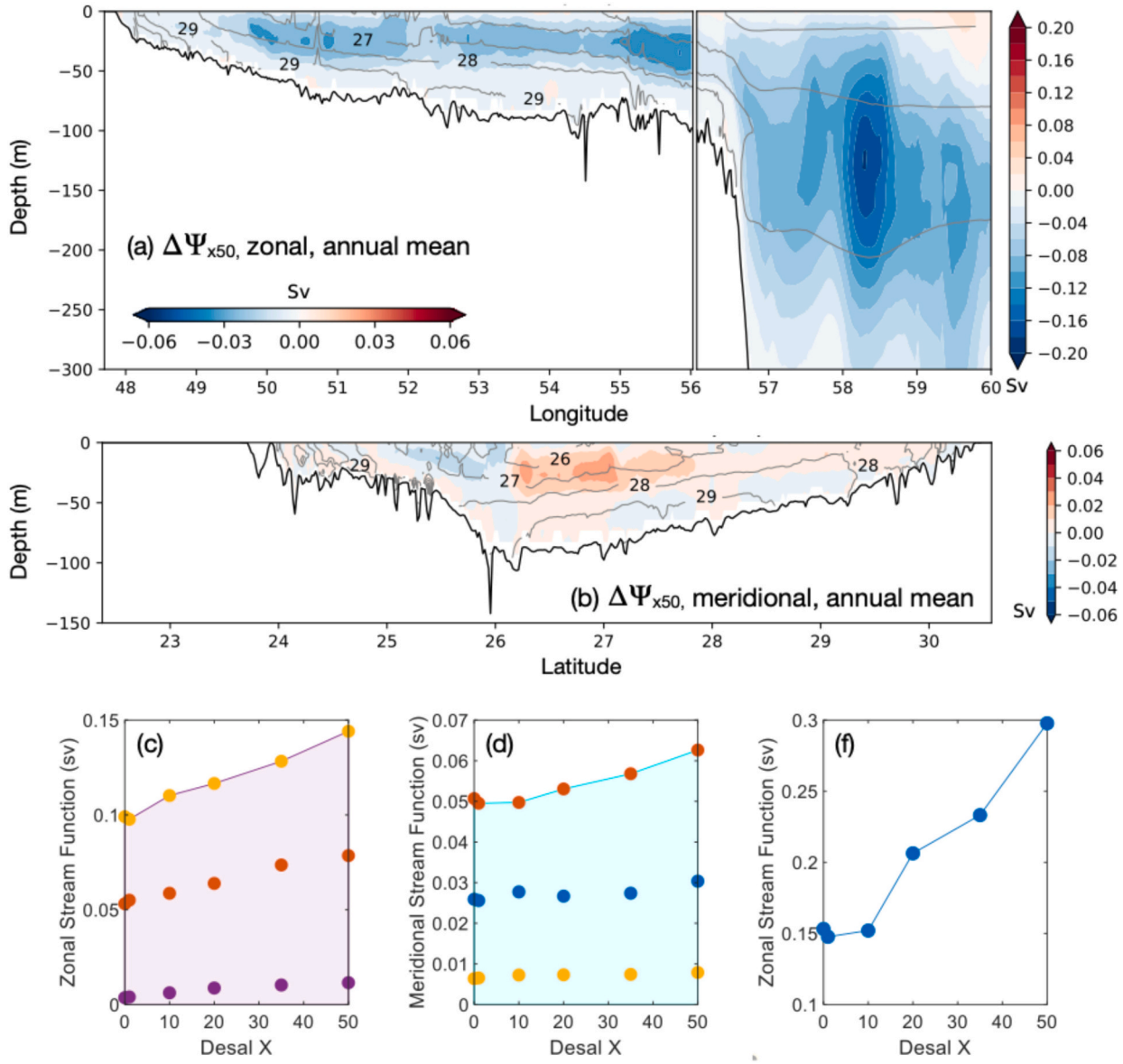

Fig. 7. The anomaly of the residual streamfunction in (a) zonal and (b) meridional directions, respectively, for ×50 compared to CTRL. There is anomalous anti-clockwise circulation around the negative anomaly of the streamfunction. (c) Zonal streamfunction (Sv) at different locations in the Arabian Gulf for CTRL, ×1, ×10, ×20, ×35 and ×50. The yellow color represents the eastern part of the Gulf, the blue color represents the center and the purple color represents the western part, (d) Meridional streamfunction (Sv) at different locations in the Arabian Gulf for CTRL, ×1, ×10, ×20, ×35 and ×50. The orange, blue and yellow dots represent the southern, central and northern part of the Gulf, and (c) the zonal stream function (Sv) at the strait of Hormuz for CTRL, ×1, ×10, ×20, ×35 and ×50. (For interpretation of the references to color in this figure legend, the reader is referred to the web version of this article.)

flow are rather robust even in extreme desalination scenarios and the salinity response, although locally large, is ameliorated on the basin scale through the efficient exchange between the Gulf and the Sea of Oman which acts to mute change.

Before concluding we should note several important limitations of our modeling framework. First, the assumption of a uniform brine recovery rate (50 %) across all desalination plants is made. In reality, recovery rates vary between plants and technologies, typically ranging from 15 % to 40 %. This could lead to an overestimation of the brine discharge volume in some regions and influence the magnitude of modeled salinity anomalies, particularly in areas with dense plant clusters. Second, the spatial distribution of desalination sources used in the model excludes several small and medium-scale plants located along the eastern and northern coasts of the Gulf. This omission may underestimate salinity buildup in these regions and lead to biased representation of localized impacts and flow anomalies. Incorporating a more complete dataset of plant locations and capacities in future models would help resolve this limitation. Third, the current model framework does not include direct thermal discharge from desalination plants. While temperature anomalies were observed near brine release zones, primarily due to salt-induced density changes and enhanced stratification, additional warming effects from the thermal component of effluent are not captured. This exclusion may lead to an underestimation of localized thermal stratification and its potential ecological implications. Fourth, the model's horizontal resolution of 2.5 km is appropriate for resolving basin-scale circulation and Gulf-wide processes but is too coarse to capture near-field plume dynamics, mixing, and localized dispersion of brine. This limitation is particularly important for ecological assessments within a few kilometers of outfalls, where fine-scale gradients are critical. Therefore, our results should be interpreted as representing large-scale and regional effects, not fine-scale local plume behavior. These limitations likely influenced the modeled

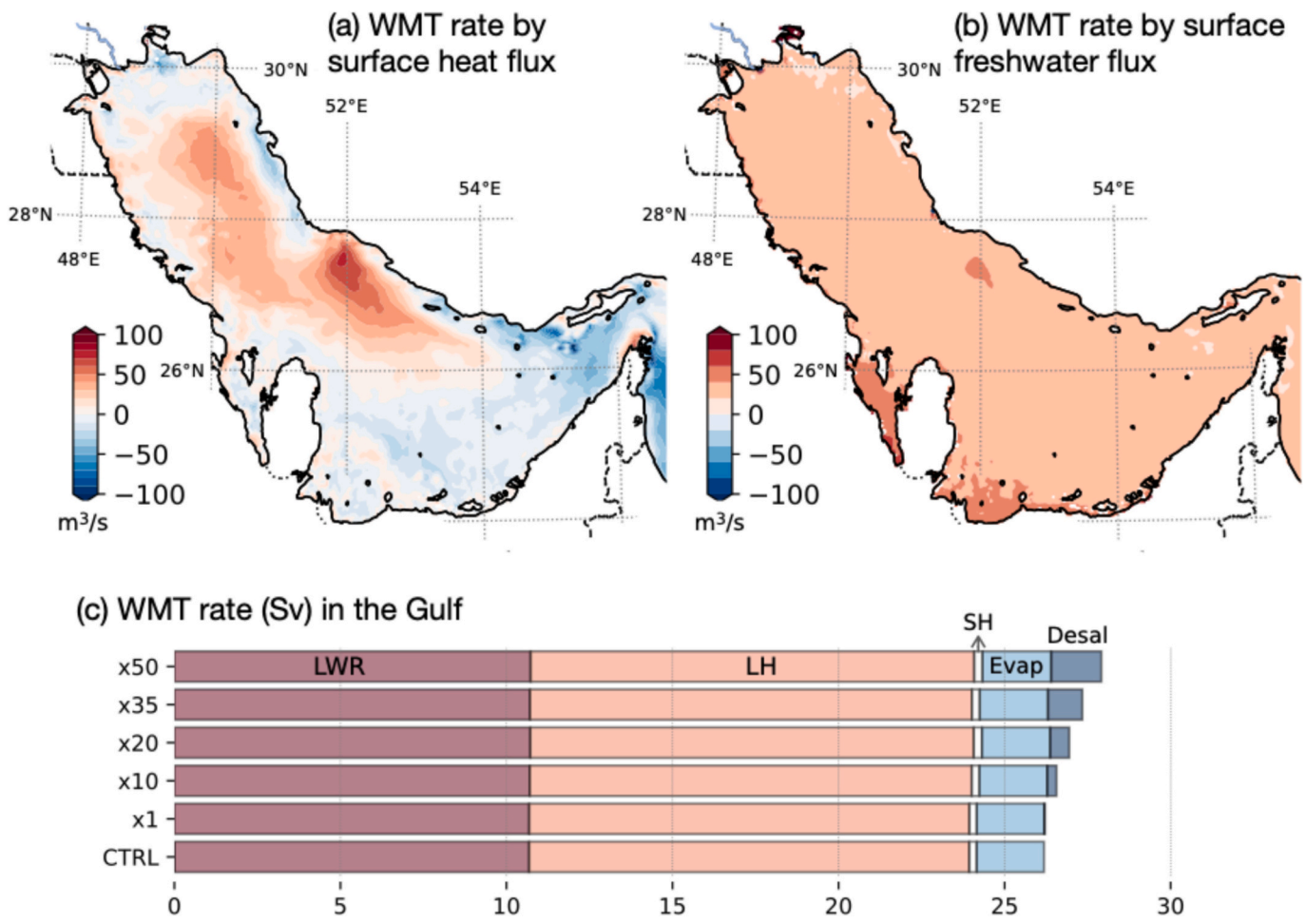

Fig. 8. Water mass transformation rate (m^3/s) by the surface (a) heat flux and (b) freshwater flux in CTRL. (c) The total water mass transformation rate by longwave radiation (LWR), latent heat flux (LH), sensible heat flux (SH), evaporation (Evap), and desalination plants (Desal) in the Gulf.

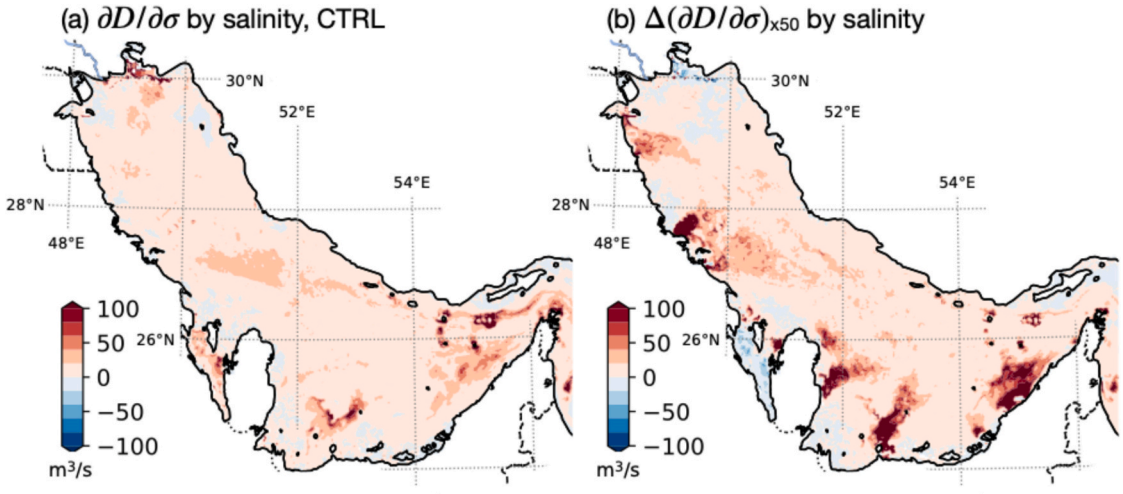

Fig. 9. (a) Transformation rate by the diffusive salt flux below the surface ($\partial D/\partial\sigma$). (b) The difference of $\partial D/\partial\sigma$ between $\times 50$ and CTRL.

spatial patterns by smoothing localized gradients and potentially underrepresenting short-term variability or interactions with smaller coastal features. Nevertheless, we believe our study provides upper-bound scenarios of desalination impacts that are robust at the regional scale.

5. Conclusions

Our study shows that notable changes in oceanographic structure, specifically in salinity, temperature, and circulation, are caused by growing desalination activities throughout the Arabian Gulf. Particularly along the southern and southwestern Gulf, dense, saline brine

discharge from coastal desalination plants promotes vertical stratification and drives localized bottom-bound density currents. Both the influx of fresher surface water and the outflow of warmer, saltier bottom water into the Sea of Oman are increased by these anomalies, which also strengthen exchange through the Strait of Hormuz and amplify the meridional and zonal overturning circulations. Due to effective flushing and water mass transformation processes, the Gulf's large-scale hydrographic characteristics are comparatively steady even when there are notable local spikes in bottom salinity, surpassing 2–3 g/kg close to outfalls. The deepening and strengthening of exchange flows act as a buffering mechanism against basin-wide impacts, even under 50-fold desalination forcing scenarios. However, persistent salinity buildup in poorly ventilated coastal regions such as the Gulf of Salwa may exceed ecological thresholds for benthic organisms. These findings suggest the need for region-specific impact assessments, improved brine dispersion strategies, and the integration of desalination expansion plans with marine environmental resilience.

Future research should include desalination plants around the entire coast of the Gulf but also prioritize a more comprehensive understanding of the long-term and cumulative impacts of desalination brine discharge on marine ecosystems, particularly on benthic and pelagic species with varying salinity tolerances. Incorporating the effects of climate change, such as rising sea temperatures and altered circulation patterns, is also critical for accurately predicting and mitigating future risks. Advanced modeling approaches, including high-resolution coupled physical-biogeochemical models, can provide deeper insights into the interplay between salinity, temperature, and marine ecology. Furthermore, exploring mitigation strategies, such as improved brine management practices and the development of less environmentally impactful desalination technologies, will be essential to balancing freshwater needs with environmental sustainability.

CRediT authorship contribution statement

Maryam R. Al Shehhi: Writing – original draft, Visualization, Validation, Methodology, Formal analysis. **Hajoon Song:** Writing – review & editing, Visualization, Validation, Methodology, Investigation, Formal analysis. **Jeffery Scott:** Writing – review & editing, Validation. **Fahim Abdul Gafoor:** Software. **John Marshall:** Writing – review & editing, Supervision, Methodology, Formal analysis, Conceptualization.

Declaration of competing interest

The authors declare that they have no known competing financial interests or personal relationships that could have appeared to influence the work reported in this paper.

Acknowledgments

The authors acknowledge Khalifa University for its generous financial support and HPC Khal-University for the Model run. JM and JS acknowledge support from MIT and the NASA Physical Oceanography program. H. Song is grateful for the support by National Research Foundation of Korea (NRF) Grant (NRF-2022R1A2C1009792) and the Korea Meteorological Administration Research and Development Program under Grant (RS-2024-00404973).

Data availability

The full LLC4320 model setup with compile-time and run-time parameters can be found at http://wwwcvs.mitgcm.org/viewvc/MITgcm/MITgcm_contrib/llc_hires/llc_4320/.

References

Alosairi, Y., Pokavanich, T., 2017. Seasonal circulation assessments of the Northern Arabian/Persian Gulf. Mar. Pollut. Bull. 116, 270–290. https://doi.org/10.1016/j.marpolbul.2016.12.065.

Alosairi, Y., Pokavanich, T., Alsulaiman, N., 2018. Three-dimensional hydrodynamic modelling study of reverse estuarine circulation: Kuwait Bay. Mar. Pollut. Bull. 127, 82–96.

Al-Shehhi, M.R., Song, H., Scott, J., Marshall, J., 2021. Water mass transformation and overturning circulation in the Arabian Gulf. J. Phys. Oceanogr. 51 (11), 3513–3527. https://doi.org/10.1175/JPO-D-21-0017.1.

Campos, E.J.D., Vieira, F., Cavalcante, G., Kjerfve, B., Abouleish, M., Shariar, S., et al., 2020. Impacts of brine disposal from water desalination plants on the physical environment in the Persian/Arabian Gulf. Environ. Res. Commun. 2, 125003.

Clark, G.F., Knott, N.A., Miller, B.M., Kelaher, B.P., Coleman, M.A., Ushiama, S., et al., 2018. First large-scale ecological impact study of desalination outfall reveals trade-offs in effects of hypersalinity and hydrodynamics. Water Res. 145, 757–768.

Danoun, R., 2007. Desalination Plants: Potential Impacts of Brine Discharge on Marine Life. The University of Technology, Sydney.

Egbert, G.D., Bennett, A.F., Foreman, M.G.G., 1994. TOPEX/POSEIDON tides estimated using a global inverse model. J. Geophys. Res. Ocean. 99, 24821–24852.

Einav, R., Harussi, K., Perry, D., 2003. The footprint of the desalination processes on the environment. Desalination 152, 141–154.

Hersbach, H., Bell, B., Berrisford, P., Hirahara, S., Horányi, A., Muñoz-Sabater, J., et al., 2020. The ERA5 global reanalysis. Q. J. Roy. Meteorol. Soc. 146, 1999–2049.

Hosseini, H., Saadaoui, I., Moheimani, N., Al Saidi, M., Al Jamali, F., Al Jabri, H., et al., 2021. Marine health of the Arabian Gulf: drivers of pollution and assessment approaches focusing on desalination activities. Mar. Pollut. Bull. 164, 112085.

Ibrahim, H.D., Eltahir, E.A.B., 2019. Impact of brine discharge from seawater desalination plants on Persian/Arabian Gulf salinity. J. Environ. Eng. 145 (12), 04019084. https://doi.org/10.1061/(ASCE)EE.1943-7870.0001604.

Ibrahim, H.D., Xue, P., Eltahir, E.A.B., 2020. Multiple salinity equilibria and resilience of Persian/Arabian Gulf basin salinity to brine discharge. Front. Mar. Sci. 7, 573.

Johns, W.E., Yao, F., Olson, D.B., Josey, S.A., Grist, J.P., Smeed, D.A., 2003. Observations of seasonal exchange through the Straits of Hormuz and the inferred heat and freshwater budgets of the Persian Gulf. J. Geophys. Res, Ocean, p. 108.

Kress, N., Gertner, Y., Shoham-Frider, E., 2020. Seawater quality at the brine discharge site from two mega-size seawater reverse osmosis desalination plants in Israel (Eastern Mediterranean). Water Res. 171, 115402. https://doi.org/10.1016/j.watres.2019.115402.

Lachkar, Z., Lévy, M., Smith, K.S., 2017. Strong intensification of the Arabian Sea oxygen minimum zone in response to Arabian Gulf water warming. Geophys. Res. Lett. 46 (10), 5420–5429.

Lattemann, S., Höpner, T., 2008. Environmental impact and impact assessment of seawater desalination. Desalination 220 (1–3), 1–15.

Le Quesne, W.J.F., Fernand, L., Ali, T.S., Andres, O., Antonpoulou, M., Burt, J.A., et al., 2021. Is the development of desalination compatible with sustainable development of the Arabian Gulf? Mar. Pollut. Bull. 173, 112940.

Marshall, J., Adcroft, A., Hill, C., Perelman, L., Heisey, C., 1997. A finite-volume, incompressible Navier Stokes model for studies of the ocean on parallel computers. J. Geophys. Res. Ocean. 102, 5753–5766. https://doi.org/10.1029/96JC02775.

Missimer, T.M., Maliva, R.G., 2018. Environmental issues in seawater reverse osmosis desalination: intakes and outfalls. Desalination 434, 198–215.

Paparella, F., D'Agostino, D., Burt, J., 2022. Long–term, basin–scale salinity impacts from desalination in the Arabian/Persian Gulf. Sci. Rep. 12, 20549.

Purnama, A., 2021. Assessing the environmental impacts of seawater desalination on the hypersalinity of Arabian/Persian Gulf. In: The Arabian Seas: Biodiversity, Environmental Challenges and Conservation Measures. Springer, pp. 1229–1245.

Rasoulpour, S., Akbari, H., 2024. Development of desalination plants within the semi-enclosed Persian Gulf. Appl. Water Sci. 14, 189.

Reynolds, R.M., 1993. Physical oceanography of the Gulf, Strait of Hormuz, and the Gulf of Oman—results from the Mt Mitchell expedition. Mar. Pollut. Bull. 27, 35–59.

Roberts, D.A., Johnston, E.L., Knott, N.A., 2010. Impacts of desalination plant discharges on the marine environment: a critical review of published studies. Water Res. 44, 5117–5128.

Rocha, C.B., Chereskin, T.K., Gille, S.T., Menemenlis, D., 2016. Mesoscale to submesoscale wavenumber spectra in Drake Passage. J. Phys. Oceanogr. 46, 601–620.

Ruso, Y.D.P., De la Ossa Carretero, J.A., Casalduero, F.G., Lizaso, J.L.S., 2007. Spatial and temporal changes in infaunal communities inhabiting soft-bottoms affected by brine discharge. Mar. Environ. Res. 64, 492–503.

Saif, O., 2012. The Future Outlook of Desalination in the Gulf: Challenges & Opportunities Faced by Qatar & the UAE. McMaster University.

Salim, M., Subeesh, M.P., Scott, J., Song, H., Marshall, J., Al Shehhi, M.R., 2024. Role of tidal mixing on ocean exchange through the Strait of Hormuz. Environ. Res. Commun. 6 (7), 071006.

Sharifinia, M., Afshari Bahmanbeigloo, Z., Smith Jr., W.O., Yap, C.K., Keshavarzifard, M., 2019. Prevention is better than cure: Persian Gulf biodiversity vulnerability to the impacts of desalination plants. Glob. Chang. Biol. 25, 4022–4033.

Shim, J.-H., Jeong, J.-Y., Park, J.-Y., 2017. SWRO brine reuse by diaphragm-type chlor-alkali electrolysis to produce alkali-activated slag. Desalination 413, 10–18.

Smith, W.H.F., Sandwell, D.T., 1997. Global sea floor topography from satellite altimetry and ship depth soundings. Science 277, 1956–1962.
Sola, I., Fernández-Torquemada, Y., Forcada, A., Valle, C., del Pilar-Ruso, Y., González-Correa, J.M., et al., 2020. Sustainable desalination: long-term monitoring of brine discharge in the marine environment. Mar. Pollut. Bull. 161, 111813.
Subeesh, M.P., Song, H., Addad, Y., Scott, J.R., Marshall, J., Al Shehhi, M.R., 2025. Seasonality of internal tides in the Strait of Hormuz: observations and modeling. J. Geophys. Res. Oceans 130 (4), e2024JC021007.
Thoppil, P.G., Hogan, P.J., 2010. Persian Gulf response to a wintertime shamal wind event. Deep Res. Part I Oceanogr. Res. Pap. 57, 946–955. https://doi.org/10.1016/j.dsr.2010.03.002.
Uddin, S., 2014. Environmental impacts of desalination activities in the Arabian Gulf. Int. J. Environ. Sci. Dev. 5, 114–117. https://doi.org/10.7763/IJESD.2014.V5.461.